

# Field independent rotational hysteresis loss on exchange coupled polycrystalline Ni-Fe/Mn-Ir bilayers

著者	角田 匡清
journal or publication title	Journal of applied physics
volume	87
number	9
page range	6415-6417
year	2000
URL	<a href="http://hdl.handle.net/10097/35370">http://hdl.handle.net/10097/35370</a>

doi: 10.1063/1.372723

# Field independent rotational hysteresis loss on exchange coupled polycrystalline Ni–Fe/Mn–Ir bilayers

Masakiyo Tsunoda<sup>a)</sup> and Migaku Takahashi

Department of Electronic Engineering, Tohoku University, Sendai 980-8579, Japan

The behaviors of the magnetic torque curve and the rotational hysteresis loss of the polycrystalline ferromagnetic (F)/antiferromagnetic (AF) bilayer whose AF layer is thinner than the critical thickness are discussed as a function of the applied field. The critical thickness of the AF layer is the threshold beyond which the unidirectional anisotropy appears. At the high field, we found some differences between the calculated torque curves based on the simple model proposed by Meiklejohn and the measured ones for the Ni–Fe/Mn–Ir bilayer: (1) the lack of the  $\sin 2\theta$  component and (2) the constant rotational hysteresis loss, in the experimental results. These differences are explained well by the model in which the two-dimensionally random distribution of the magnetic anisotropy axes of the AF grains is taken into account. We conclude the distribution of the anisotropy axes of the AF grains is an indispensable factor to understand the unidirectional anisotropy of the polycrystalline F/AF bilayers. © 2000 American Institute of Physics. [S0021-8979(00)85608-X]

## I. INTRODUCTION

The unidirectional anisotropy<sup>1</sup> of exchange coupled ferromagnetic (F)/antiferromagnetic (AF) bilayers is important for applications in spin valves,<sup>2</sup> however, the origin of this phenomenon is not yet fully understood. Some of the important questions concerning the mechanism of the unidirectional anisotropy include the magnetic anisotropy of the AF layer and the role of it on the magnetization process of the F layer. According to the simple model proposed by Meiklejohn (hereafter, single spin model),<sup>1,3</sup> when the AF layer thickness ( $d_{AF}$ ) is less than the critical value ( $d_{AF}^{cr}$ , beyond which an exchange biasing field appears), the axis of the AF spins follows close to the magnetization of the F layer, which is rotating with the large applied field.<sup>4</sup> It is therefore expected to determine the magnetic anisotropy of the AF layer from the magnetic torque measurements of the F/AF bilayers ( $d_{AF} < d_{AF}^{cr}$ ). However, we recently found some significant differences between the behavior of the calculated magnetic torque curve against the applied field (based on the single spin model) and that of the measured one for the exchange coupled Ni–Fe/Mn–Ir bilayers.<sup>4</sup> The most probable cause of these differences is the too simplified description in the single spin model—the magnetic anisotropy of the AF layer, which is *unified in the whole film plane*.<sup>1,3</sup> In this article, in order to comprehend the behaviors of the measured torque curve and the rotational hysteresis loss of the F/AF bilayers ( $d_{AF} < d_{AF}^{cr}$ ), we establish a new model by expanding the single spin model to fit to the actual bilayer system precisely.

## II. EXPERIMENT

Substrate/Ta 50 Å/Ni–Fe 50 Å/Mn<sub>59</sub>Ir<sub>41</sub>  $d_{AF}$ /Ta 50 Å quadrilayered films were prepared under the extremely clean sputtering process.<sup>4–6</sup> The critical thickness of the antiferromagnetic Mn–Ir layer,  $d_{AF}^{cr}$ , was 37 Å, where the exchange

biasing field steeply increased.<sup>4</sup> The magnetic torque curves were measured for as-deposited films with null method torque magnetometer having a sensitivity of about  $1 \times 10^{-3}$  dyn cm. The magnitudes of  $\sin \theta$  and  $\sin 2\theta$  components of the torque curve were determined from Fourier analysis of it. The rotational hysteresis loss was determined as a half of the area enclosed by both torque curves for the clockwise ( $\theta: 0 \rightarrow 2\pi$ ) and for the counter-clockwise ( $\theta: 2\pi \rightarrow 0$ ) rotation.

Figure 1 shows the results determined from the measured magnetic torque curves on Ni–Fe 50 Å/Mn–Ir 30 Å bilayer. The magnitudes of the  $\sin \theta$  and the  $\sin 2\theta$  components, and the rotational hysteresis loss are plotted against

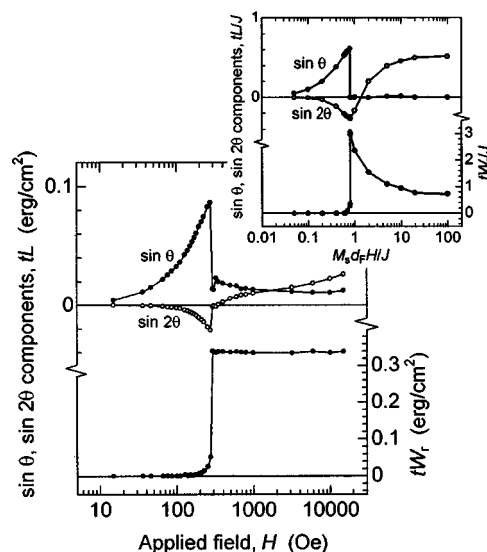


FIG. 1. The magnitudes of  $\sin \theta$ ,  $\sin 2\theta$  components and the rotational hysteresis loss,  $tW_r$ , of the measured torque curves for Ni–Fe 50 Å/Mn–Ir 30 Å bilayer as a function of the applied field. The values are indicated per unit area of the film plane. The inset shows the corresponding calculated results based on the single spin model.

<sup>a)</sup>Electronic mail: tsunoda@ecei.tohoku.ac.jp

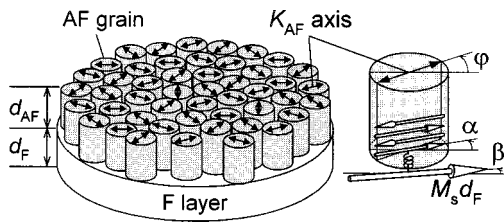


FIG. 2. A schematic model of the F/AF bilayer. The spin configuration in the F layer and in the AF grain, and the angular relations of them are indicated (right).

the applied field,  $H$ . The inset shows the results determined from the calculated torque curves,<sup>4</sup> based on the single spin model. The calculation parameter was  $K_{AF}d_{AF}/J=0.8$ , which corresponds to the experimental results of  $d_{AF}=30 \text{ \AA}$  case (cf.  $d_{AF}^{cr} \equiv J/K_{AF}=37 \text{ \AA}$ ). Here,  $J$  is the coupling energy per unit area of the interface between the F and the AF layers.

As the measured results in Fig. 1, the magnitude of the  $\sin \theta$  component gradually becomes large with increasing the applied field up to 280 Oe, then drops abruptly. With further increasing field, it decreases slightly but remains nonzero. The magnitude of the  $\sin 2\theta$  component increases gradually in the opposite sign to the  $\sin \theta$  component, up to 280 Oe, then abruptly becomes to zero. With further increasing field, it scarcely increases, changing its sign, but remains small. On the other hand, the rotational hysteresis loss,  $tW_r$ , increases slightly until  $H=280 \text{ Oe}$ , then discontinuously jumps to  $0.34 \text{ erg/cm}^2$ , and remains constant with further increasing field. Comparing these experimental results to the calculated ones (the inset in Fig. 1), we find some disagreements between them at the high field. Namely, in the experimental results, (a) the  $\sin \theta$  component persists; (b) the  $\sin 2\theta$  component remains small (less than one-third of the peak value of the  $\sin \theta$  component); (c)  $tW_r$  remains constant. The origin of the disagreement (a) is due to the deviation of the AF layer thickness in the actual bilayer.<sup>4</sup> The main purpose of this paper is to establish the new model which explains the disagreements (b) and (c).

From the microstructural analysis, we found that the present bilayers have polycrystalline structure and that the Mn-Ir grains have no preferred orientation in the film plane.<sup>7</sup> By assuming the magnetocrystalline anisotropy of the AF grains as an origin of the magnetic anisotropy of the AF layer, we should take into account the random distribution of the anisotropy axes of the AF grains in the calculation model.

### III. MODELING

Figure 2 shows the schematic model of the F/AF bilayer. The F layer is regarded as a single domain (i.e., the magnetization of the F layer is treated as a single spin). The AF layer is regarded as an aggregation of the AF grains whose magnetocrystalline anisotropy has uniaxial symmetry. The anisotropy axes of the AF grains lie in the film plane with two-dimensionally random distribution. Here, we assume that

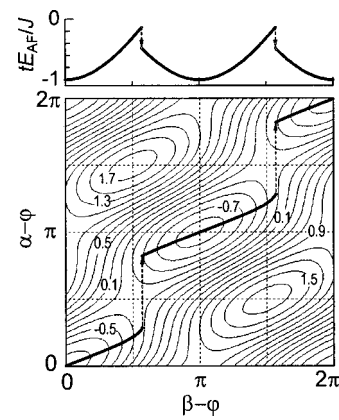


FIG. 3. A contour map of the AF grain's energy as functions of deviation angles  $\alpha-\varphi$  and  $\beta-\varphi$ , calculated for the case of  $K_{AF}d_{AF}/J=0.8$ . The contour lines indicate the reduced energy,  $tE_{AF}/J$ . The upper part shows the change of  $tE_{AF}/J$  along the thick lines in the contour map.

the intergranular magnetic coupling of the AF grains is neglected and that the single spin model is applicable between the F layer and each AF grain.

In order to calculate the torque curves of this F/AF system, we first consider the energy of an AF grain per unit area of the film plane:

$$tE_{AF} = K_{AF}d_{AF} \sin^2(\alpha - \varphi) - J \cos(\alpha - \beta), \quad (1)$$

where,  $K_{AF}d_{AF}$  is the magnetocrystalline anisotropy energy of the AF grain per unit area of the film plane;  $J$  is the coupling energy per unit area of the F/AF interface; angle  $\varphi$  is the direction of the anisotropy axis of the AF grain, which is defined in the range from  $-\pi/2$  to  $\pi/2$ ; angles  $\alpha$  and  $\beta$  are the directions of the axis of the AF spins and the magnetization of the F layer, respectively. From the partial derivation of Eq. (1) with  $\alpha$ , we obtain the energy minimum equations, which determine the angle  $\alpha$  under the certain values of  $\beta$  and  $\varphi$ .

Figure 3 shows a contour map of the AF grain's energy as functions of deviation angles  $\alpha-\varphi$  and  $\beta-\varphi$ , calculated with Eq. (1) for the case of  $K_{AF}d_{AF}/J=0.8$ . The reduced energy,  $tE_{AF}/J$ , is indicated by contour lines. Thick lines in the map indicate the loci of the angle  $\alpha-\varphi$  which satisfying the energy minimum equations, when the angle  $\beta-\varphi$  continuously changes from 0 to  $2\pi$  (clockwise rotation). The change of the reduced energy,  $tE_{AF}/J$ , along the loci is also indicated in the upper part of Fig. 3, as a function of the angle  $\beta-\varphi$ .

Here, we confine the discussion to the case of  $\varphi=0$  for simplification. When the direction of the F layer magnetization  $\beta=0$ , the direction of the AF spin axis  $\alpha=0$ . With increasing  $\beta$  up to  $0.57\pi$ ,  $\alpha$  follows behind  $\beta$  and becomes  $0.28\pi$ . At the same time,  $tE_{AF}/J$  increases from  $-1$  to  $-0.14$ . Then  $\alpha$  discontinuously jumps to the new angle  $0.82\pi$ , and the energy portion of the AF grain is released irreversibly (dashed arrows in the figure). With further increasing  $\beta$  to  $\pi$ ,  $\alpha$  precedes  $\beta$  and gradually increases to  $\pi$ . In the region,  $\pi \leq \beta \leq 2\pi$ , we can see a similar change of  $\alpha$  against increasing  $\beta$ . From these results, one can say that the AF grain exhibits twofold symmetry in its magnetic potential

energy for a round rotation of the F layer magnetization. Extending the discussion to the case of AF grains with  $\varphi \neq 0$ , one can clearly say that the changes of both  $\alpha$  and  $tE_{AF}/J$  against  $\beta$  is identical to those of the  $\varphi=0$  case, except for the phase shift  $\varphi$  on  $\alpha$  and  $\beta$ .

With these points in mind, next step, we discuss the configuration of  $\alpha$ 's of the respective AF grains and the total energy of them for a certain value of  $\beta$ . When  $\beta=\pi/2$ , the deviation angles  $\beta-\varphi$  uniformly distribute from 0 to  $\pi$ , because  $\varphi$ 's of the AF grains uniformly distribute in the region  $-\pi/2 \leq \varphi \leq \pi/2$  (two-dimensionally random). Corresponding with the respective angles of  $\beta-\varphi$ , the angles  $\alpha-\varphi$  distribute from 0 to  $0.28\pi$  and from  $0.82\pi$  to  $\pi$ , along the loci in Fig. 3; the summed up energy of all the AF grains is given as the integral of  $tE_{AF}/J$  about  $\beta-\varphi$  from 0 to  $\pi$ .

Since  $tE_{AF}/J$  has twofold symmetry and the integrating width of  $\beta-\varphi$  is always  $\pi$ , the summed up energy of all the AF grains does not change when  $\beta$  changes. This result means that the AF grains cause no magnetic anisotropy on the F layer magnetization.

We should notice the balance of energy in the system. While the F layer magnetization makes one rotation, each AF grain changes its spin angle  $\alpha$  discontinuously and releases the energy portion irreversibly, twice (see Fig. 3). The total energy released by all the AF grains corresponds to the rotational hysteresis loss,  $tW_r$ . On the other hand, the energy supplied from the field  $H$  to the system under a round rotation of the F layer magnetization is  $M_s d_F H \sin(\theta-\beta) \times 2\pi$ , where  $\theta-\beta$  is the deviation angle between the field and the magnetization. Only when the supplying energy is greater than the releasing energy, the F layer magnetization can rotate. We thus obtain the condition to rotate the F layer magnetization:  $M_s d_F H \geq tW_r / (2\pi)$ . Under the field satisfying  $M_s d_F H < tW_r / (2\pi)$ , the F layer magnetization is adhered to the preferred direction  $\beta_0$ , which is determined by the magnetic anisotropy of the F layer and many other factors. As a result, the magnetic torque  $M_s d_F H \sin(\theta-\beta_0)$ , is observed without the rotational hysteresis loss.

Figure 4 represents the quantitatively calculated results for various  $K_{AF}d_{AF}/J$  values. The  $\sin \theta$  component and the rotational hysteresis loss are plotted against the reduced ap-

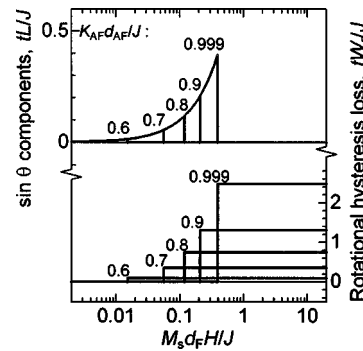


FIG. 4. The magnitude of  $\sin \theta$  component and the rotational hysteresis loss of the calculated torque curves for various  $K_{AF}d_{AF}/J$  values as a function of the reduced applied field.

plied field,  $M_s d_F H / J$ . When  $K_{AF}d_{AF}/J=0.8$ , the reduced  $\sin \theta$  component,  $tL/J$ , linearly increases with increasing  $M_s d_F H / J$  up to 0.12, then abruptly vanishes. At the same field, the reduced rotational hysteresis loss,  $tW_r/J$ , suddenly appears, and beyond which  $tW_r/J$  keeps constant value of 0.74. One can fairly say that these behaviors qualitatively agree with the measured ones, shown in Fig. 1. Namely, the differences (b) and (c) mentioned in the preceding section are well explained by the present model.

From all the measured and the calculated results, we conclude that the distribution of the anisotropy axes of the AF grains is an indispensable factor to understand the unidirectional anisotropy of the polycrystalline F/AF bilayers.

- <sup>1</sup>W. H. Meiklejohn and C. P. Bean, Phys. Rev. **102**, 1413 (1956); **105**, 904 (1957).
- <sup>2</sup>B. Dieny, V. S. Speriosu, S. S. P. Parkin, B. A. Gurney, D. R. Wilhoit, and D. Mauri, Phys. Rev. B **43**, 1297 (1991).
- <sup>3</sup>W. H. Meiklejohn, J. Appl. Phys. **33**, 1328 (1962).
- <sup>4</sup>M. Tsunoda, Y. Tsuchiya, T. Hashimoto, and M. Takahashi, J. Appl. Phys. (in press).
- <sup>5</sup>M. Tsunoda, K. Uneyama, T. Suzuki, K. Yagami, and M. Takahashi, J. Appl. Phys. **85**, 4919 (1999).
- <sup>6</sup>K. Okuyama, T. Shimatsu, S. Kuji, and M. Takahashi, IEEE Trans. Magn. **31**, 3838 (1995).
- <sup>7</sup>K. Yagami, M. Tsunoda, and M. Takahashi, J. Appl. Phys. **87**, (2000), these proceedings.